IVYSPRING INTERNATIONAL PUBLISHER

Theranostics

2016; 6(12): 2225-2234. doi: 10.7150/thno.16260

Research Paper

In Vitro and *In Vivo* Evaluation of ^{89}Zr-DS-8273a as a Theranostic for Anti-Death Receptor 5 Therapy

Ingrid J.G. Burvenich[1,2#], Fook-Thean Lee[1,2#], Nancy Guo[1], Hui K. Gan[1,2,4], Angela Rigopoulos[1,2], Adam C. Parslow[1,2], Graeme J. O'Keefe[4,5], Sylvia J. Gong[5,6], Henri Tochon-Danguy[5], Stacey E. Rudd[7], Paul S. Donnelly[7], Masakatsu Kotsuma[8], Toshiaki Ohtsuka[9], Giorgio Senaldi[10] and Andrew M. Scott[1,2,3,4,5]✉

1. Tumour Targeting Laboratory, Olivia Newton-John Cancer Research Institute, Melbourne, Australia;
2. School of Cancer Medicine, La Trobe University, Melbourne, Australia;
3. Department of Medicine, University of Melbourne, Melbourne, Australia;
4. Department of Medical Oncology, Austin Health, Heidelberg, Melbourne, Australia;
5. Department of Molecular Imaging and Therapy, Austin Health, Melbourne, Australia;
6. School of Engineering and Mathematical Sciences, La Trobe University, Melbourne, Australia;
7. School of Chemistry and Bio21 Molecular Science & Biotechnology Institute, University of Melbourne, Melbourne, Australia.
8. Translational Medicine & Clinical Pharmacology Department, Daiichi Sankyo Co Ltd, Tokyo, Japan;
9. Biologics Pharmacology Research Laboratories, Daiichi Sankyo Co Ltd, Tokyo, Japan.
10. Department of Translational Medicine and Clinical Pharmacology, Daiichi Sankyo Pharma Development, Edison, NJ, USA.

#Authors contributed equally to this work.

✉ Corresponding author: Professor Andrew M. Scott, Tumour Targeting Laboratory, Olivia Newton-John Cancer Research Institute, 145-163 Studley Road, Heidelberg, Victoria 3084, Australia. Phone: 61-39496-5876; Fax: 61-39496-5334; E-mail: andrew.scott@onjcri.org.au.

Received: 2016.05.23; Accepted: 2016.08.28; Published: 2016.09.25

Abstract

Background: DS-8273a, an anti-human death receptor 5 (DR5) agonistic antibody, has cytotoxic activity against human cancer cells and induces apoptosis after specific binding to DR5. DS-8273a is currently being used in clinical Phase I trials. This study evaluated the molecular imaging of DR5 expression *in vivo* in mouse tumor models using SPECT/CT and PET/MRI, as a tool for drug development and trial design. **Methods:** DS-8273a was radiolabeled with indium-111 and zirconium-89. Radiochemical purity, immunoreactivity, antigen binding affinity and serum stability were assessed *in vitro*. *In vivo* biodistribution and pharmacokinetic studies were performed, including SPECT/CT and PET/MR imaging. A dose-escalation study using a PET/MR imaging quantitative analysis was also performed to determine DR5 receptor saturability in a mouse model. **Results:** ^{111}In-CHX-A″-DTPA-DS-8273a and ^{89}Zr-Df-Bz-NCS-DS-8273a showed high immunoreactivity (100%), high serum stability, and bound to DR5 expressing cells with high affinity (K_a, 1.02-1.22 × 10^{10} M^{-1}). The number of antibodies bound per cell was 32,000. *In vivo* biodistribution studies showed high and specific uptake of ^{111}In-CHX-A″-DTPA-DS-8273a and ^{89}Zr-Df-Bz-NCS-DS-8273a in DR5 expressing COLO205 xenografts, with no specific uptake in normal tissues or in DR5-negative CT26 xenografts. DR5 receptor saturation was observed *in vivo* by biodistribution studies and quantitative PET/MRI analysis. **Conclusion:** ^{89}Zr-Df-Bz-NCS-DS-8273a is a potential novel PET imaging reagent for human bioimaging trials, and can be used for effective dose assessment and patient response evaluation in clinical trials.

Key words: DS-8273a, death receptor 5, apoptosis, zirconium-89, colorectal cancer, PET/MRI.

Introduction

Death receptor 5 (DR5) is a member of the tumor necrosis factor (TNF) receptor superfamily. TNF-related apoptosis-inducing ligand (TRAIL), its endogenous ligand, can trigger an apoptosis signal upon binding DR5, causing cell death in a wide variety of tumor cell lines [1, 2]. Effective apoptosis induction by DR5-targeting TRAIL or antibodies have been reported in mouse models of leukemia, multiple myeloma, melanoma, breast, bladder, prostate, renal and colon cancer, either as monotherapy and/or as

combination therapy with chemotherapeutic agents [2]. Although DR5 agonists have been shown to be safe and well tolerated in patients, their respective anticancer activities have been largely disappointing [3, 4]. Second generation TRAIL receptor targeting agents with increased bioactivity are currently being developed with the aim to improve the outcome of TRAIL-based therapies [5].

Although DR5 expression is increased in malignant cells compared to normal tissue, immunohistochemical studies have shown expression of DR5 in normal colon mucosa as well as colorectal adenomas and carcinomas [6]. However, normal cells are relatively resistant to DR5 signaling [1]. Therefore, TRAIL or agonistic anti-DR5 antibodies might be of therapeutic benefit in the treatment of colon cancer patients [7].

CS-1008 (Tigatuzumab) is a humanized monoclonal IgG1 with agonistic activity upon binding to human DR5 [8]. It was developed by Daiichi Sankyo CO. Ltd. (Tokyo, Japan) from a murine anti-DR5 monoclonal antibody, TRA-8 (mTRA-8), by complementarity determining region grafting [9]. CS-1008 causes cell death in various DR5 expressing human tumor cell lines via apoptosis induction and its potency is augmented by cross-linking [8]. In contrast to other anti-DR5 antibodies and TRAIL, CS-1008 did not show cytotoxicity in human primary hepatocytes [8, 10, 11]. As a monotherapy, anti-tumor efficacy was seen in COLO 205 colon tumors and MIA PaCa-2 pancreatic tumors. Limited anti-tumor activity was seen with NCI-H2122 lung tumors, although combination treatment with gemcitabine showed significant anti-tumor response [8]. A phase I clinical trial demonstrated that CS-1008 was well tolerated at doses as high as 8 mg/kg/week, dose limiting toxicity was not seen and maximum tolerated dose was not reached [12]. The best response to therapy was long-term disease stabilization. Although this is supportive of the clinical potential of a DR5 targeting antibody, strategies to improve the potency of DR5 antibodies is clearly justified.

^{111}In-CHX-A″-DTPA-CS-1008 was developed and characterised as a diagnostic tool to evaluate the DR5 receptor occupancy *in vivo* through molecular imaging [13]. DR5 imaging with ^{111}In-CHX-A″-DTPA-CS-1008 in a phase I imaging and pharmacodynamic trial revealed interpatient and intrapatient heterogeneity of tumor uptake [14]. ^{111}In-CHX-A″-DTPA-CS-1008 uptake in tumor was not dose dependent, but importantly was predictive of clinical benefit in the treatment of patients who had metastatic colorectal cancer [14].

DS-8273 is a newly generated humanized IgG1 DR5 agonistic antibody with different amino acid sequences in complementarity determining regions from CS-1008, generated by Daiichi Sankyo. Here we report the radiolabeling of DS-8273a via bifunctional chelates C-functionalized *trans*-cyclohexyldiethylene-triaminepentaacetic acid (CHX-A″-DTPA) and *p*-isothiocyanatobenzyl-desferrioxamine (Df-Bz-NCS) to indium-111 (^{111}In) and zirconium-89 (^{89}Zr) respectively, suitable for *in vivo* molecular imaging with single photon emission computed tomography (SPECT, ^{111}In) and positron emission computed tomography (PET, ^{89}Zr). ^{111}In-CHX-A″-DTPA-DS-8273a and ^{89}Zr-Df-Bz-NCS-DS-8273a were compared *in vitro* and in an animal mouse model, with the aim to select the best reagent for use in human bioimaging studies. A non-invasive tracer may inform the clinical development of DS-8273a through dose selection and patient response assessment.

Materials and Methods

Cell Culture

The human DR5-positive colorectal carcinoma cell line COLO 205 and mouse DR5-negative cell line CT26 were obtained from the American Type Culture Collection (ATCC, Manassas, MD, USA). The cells were cultured in RPMI (Invitrogen, Carlsbad, CA, USA) with 10% fetal calf serum, 2mM GlutaMAX (Gibco), and 100 units/mL of penicillin and 100 µg/mL of streptomycin in a 10 mM citrate buffer (Gibco), incubated at 37°C with 5% CO_2.

Chelation of CHX-A″-DTPA and Df-Bz-NCS to DS-8273a for radiolabeling

Analytical grade reagents, sterile technique and pyrogen-free plasticware were used in all labeling steps. DS-8273a was provided by Daiichi Sankyo Co., Ltd. (Tokyo, Japan).

DS-8273a was chelated with the bifunctional metal ion chelator, C-functionalized trans-cyclohexyl-diethylenetriaminepentaacetic acid (CHX-A″-DTPA; Macrocyclics Inc, Dallas, TX, USA) at 5.0-fold molar excess as described before [13]. Before chelation, DS-8273a was dialyzed against 50 mM sodium bicarbonate buffer (Na_2CO_3, pH 8.6) containing 150 mM NaCl and 3g/L of Chelex-100 (Biorad, Australia) for 6 hours with change of buffer, and then overnight at 4°C. Chelate was added to DS-8273a and incubated at room temperature, with frequent gentle mixing for an hour, then overnight in the dark. Excess unbound antibody was removed by 6 h dialysis with 20 mM sodium acetate buffer containing 0.15 M NaCl (pH 6.3) and 3 g/L of Chelex-100, followed by overnight dialysis at 4°C with one change of buffer. Aliquots of 1 mg were stored at -80°C in dialysis buffer.

DS-8273a was chelated with *p*-isothiocyanatobenzyl-desferrioxamine (Df-Bz-NCS; Macrocyclics Inc) at a 3.0-fold molar excess similarly as described before [13, 14]. Before chelation, 100 mg of DS-8273a was dialysed twice against 100 mM sodium bicarbonate buffer (Na145-$_2CO_3$, pH 8.6) containing 0.15 M NaCl and 3 g/L of Chelex-100. Chelate solution (3.8 mg/mL in DMSO) was incubated with antibody for 6 hours at room temperature with mixing. Purification of Df-Bz-NCS-DS-8273a was done overnight via dialysis against 0.01% Tween-80/ 0.5% DMSO/chelex-100 phosphate-buffered saline with 2 changes of buffer at 4°C. Conjugates were stored in 2.0 mg aliquots at -80°C until required.

Radiolabeling and Quality Assurance

Post chelation, DS-8273a was trace radiolabeled as follows: For ^{111}In-CHX-A″-DTPA-DS-8273a, 200 µL containing 137.64 MBq (3.72 mCi) of ^{111}In (Mallinckrodt Australia Pty Ltd, Sydney, Australia) was neutralised with 40 µL of 0.5 M sodium acetate solution and mixed with 1.0 mg CHX-A″-DTPA-DS-8273a for 20 minutes, followed by 32 µL of 10 mM EDTA (pH 4.5). Resultant mixture was purified by Sephadex G50 chromatography equilibrated and eluted in saline. For ^{89}Zr-Df-Bz-NCS-DS-8273a, 100 µL ^{89}Zr in oxalic acid (PerkinElmer, Melbourne, Australia) with 45 µL of 2 M sodium carbonate and after 3 minutes, 150 µL of 1 M HEPES buffer (pH 7.2) was added and the solution was sterile filtered. The filtrate containing 75 MBq (2.0 mCi) of ^{89}Zr was mixed with 1.0 mg Df-Bz-NCS-DS-8273a, followed by addition of 240 µL of 1 M HEPES buffer. The mixture was incubated at room temperature for 45 minutes. Finally, 10 mM EDTA was added to a final concentration of 1 mM before purification. Radiolabeled products were purified on a Sephadex G50 column (Pharmacia, Uppsala, Sweden) equilibrated with sodium chloride injection BP 0.9% w/v (Pfizer, Sydney, Australia).

Radiochemical purity was estimated by instant thin layer chromatography [13]. Lindmo assay and Scatchard analysis were performed as described before [13]. The immunoreactivity (IR) of radiolabeled DS-8273a to COLO 205 target cells was determined by linear extrapolation to binding at infinite antigen excess using a Lindmo assay [13]. The percentage of binding of DS-8273a to COLO 205 cells was calculated by the formula: (cpm cell pellet/mean cpm radioactive antibody standards) × 100. The percentage of binding was graphed against COLO 205 cell concentration using Graphpad Prism version 6.03 (www.graphpad.com), and IR was calculated as the Y-intercept of the inverse plot of both values. Scatchard analysis was used to calculate the apparent association constant (K_a) and number of antibody molecules bound per cell [13]. The IR fraction was taken into account in calculating the amount of free, reactive antibody [(100 × % bound)/100 × total antibody × IR fraction], and specific binding (nM; total antibody × % bound) was graphed against specific binding/reactive free. The association constant was determined from the negative slope of the line. The number of DS-8273a molecules bound per cell was derived by: [(X-intercept of Scatchard plot (nM) × 10^{-9}/1000) × (6.023 × 10^{23})]/number of cells used in the assay (5 × 10^6). Serum stability was assessed by incubating 10 µg ^{111}In-CHX-A″-DTPA-DS-8273a or 10 µg ^{89}Zr-Df-Bz-NCS-DS-8273a in 100 µL of human serum at 37°C for a 7-day period. Radiochemical purity and single-point immunoreactivity assays at 0 (day of radiolabeling, no incubation), 2 and 7 days of incubation were performed with COLO 205 cells (5 × 10^6) as described before [13]. Radioconstruct integrity was assessed by Size Exclusion Chromatography (SEC) [13]. The constructs were analysed by fast liquid protein chromatography (FPLC) before and after labeling to determine the integrity of the radiolabeled proteins. The samples were eluted isocratically on a Superdex 200 HR 10/30 column (Amersham Pharmacia) using phosphate buffered saline (pH 7.4) at a flow rate of 0.2 mL/min. Eluted radiolabeled antibodies were detected by UV absorbance at 280 nm by a Beckman System Gold detector (Beckman Instruments, Fullerton, *CA), and radioactivity was measured by Packard Radiomatic Flo One (Packard Instruments).

Animal Model

In vivo investigations were performed in 5-6 week old female athymic BALB/c *nu/nu* mice (Animal Research Centre, WA, Australia). All animal studies were approved by the Austin Hospital Animal Ethics Committee and were conducted in compliance with the Australian Code for the care and use of animals for scientific purposes. To establish tumors, mice were injected subcutaneously into the left underside flank with DR5-positive COLO 205 cells (2 × 10^6 cells) or negative murine CT26 cells (1 × 10^6 cells) in a total volume of 0.1 mL phosphate-buffered saline. Tumor volume (TV) was calculated by the formula [(length × width^2)/2] where length was the longest axis and width the measurement at right angles to length.

Biodistribution Study with ^{111}In- and ^{89}Zr-labeled DS-8273a

In a first biodistribution study, BALB/c *nu/nu* mice with established COLO 205 xenografts (TV = 468

- 657 mg) or CT26 (TV = 518 - 618 mg) received a dose of 0.2886 MBq ^{111}In-CHX-A″-DTPA-DS-8273a (5 µg, 7.8 µCi), intravenously via the tail vein (0.1 mL). In a second biodistribution study, BALB/c *nu/nu* mice with established COLO 205 (TV range = 218 to 684 mg) or CT26 xenografts (TV range = 182 to 775 mg) received a dose of 0.305 MBq ^{89}Zr-Df-Bz-NCS-DS-8273a (5.0 µg, 8.25 µCi), intravenously via the tail vein (0.1 mL). On day 0 (2 hours), 1, 2, 3, 5, 7 and 10 after injection, groups of mice bearing COLO 205 tumors (n = 5) were sacrificed and biodistribution of radiolabeled DS-8273a was assessed as described before [13]. For mice bearing DR5-negative CT26 xenografts, biodistribution was only assessed on day 2 post injection. The tissue distribution data were calculated as the mean ± SD percent injected dose per gram tissue (%ID/g) for the radiolabeled constructs per time point.

Serum from blood collected from COLO 205 tumor-bearing mice injected with radiolabeled antibody was used to determine pharmacokinetic parameters as described before [13].

Animal Imaging with ^{111}In- and ^{89}Zr-labeled DS-8273a

In order to perform *in vivo* SPECT/CT imaging of ^{111}In-labeled DS-8273a, a separate group of 2 mice received a higher dose of 4.07 MBq ^{111}In-CHX-A″-DTPA-DS-8273a (70.5 µg, 110.0 µCi) and were imaged with single photon emission tomography (SPECT) and computed tomography (CT) on days 0 (2 hours), 3 and 7 after injection on a nanoSPECT/CT camera (nanoScan®, Mediso). *In vivo* PET imaging of ^{89}Zr-labeled DS-8273a was performed on a separate group of 5 COLO 205 tumor-bearing mice receiving a dose of 2.775 MBq ^{89}Zr-Df-Bz-NCS-DS-8273a (45.5 µg, 75 µCi). Mice were imaged with positron emission tomography (PET) and computed tomography (CT) on days 0 (2 hours), 2 and 7 on a small animal nanoPET/MR camera (nanoScan®, Mediso, Budapest, Hungary).

Imaging DR5 Saturation *In Vivo* with ^{89}Zr-labeled DS-8273a

The influence of DS-8273a protein dose on tumor uptake and DR5 saturation *in vivo* was determined in a separate biodistribution and PET/MR imaging study using ^{89}Zr-Df-Bz-NCS-DS-8273a. For the biodistribution study, three groups of mice (n = 5) were injected with 0.3441 MBq ^{89}Zr-Df-Bz-NCS-DS-8273a (4.6 µg, 9.3 µCi) combined with different amounts of unlabeled DS-8273a to achieve a total protein dose of 0.3, 3, and 30 mg/kg in a total volume of 0.1 mL 0.9% w/v of sodium chloride. On day 2 and day 7 after injection, all animals were sacrificed and organs were collected as described above. The tissue distribution data was calculated as the mean ± SD %ID/g. To assess the therapeutic effect of DS-8732a at the different dose levels *in vivo*, tumor volumes were measured on day 0 (2 hours), 2 and 7 prior to being sacrificed for biodistribution study on day 7.

In parallel, 1-2 mice of each group were imaged on day 0 (2 hours), 2 and 7 post injection using the small animal nanoPET/MR camera (nanoScan®, Mediso, Budapest, Hungary). Imaging analysis was performed on the series of PET/MR images acquired. Tumor uptake (kBq/cc) was determined by mark-up of volumes of interest (VOI) in cross-sectional PET images. Tumor volume (mL) was determined based on mark-up of VOI in cross-sectional MR images. To convert (kBq/cc)/mL to %ID/mL, total body uptake (kBq/cc) in each mouse was measured on day 0 as an approximation of injected dose (ID).

Statistical Analyses

An unpaired t-test was used to determine significant differences of pharmacokinetic parameters calculated for ^{111}In- and ^{89}Zr-labeled DS-8273a antibody. For multiple comparisons, one-way ANOVA was used. All analyses were done using Graphpad Prism version 6.03. Data are presented as the average ± SD, unless stated differently.

Results

Conjugation, Radiolabeling and Quality Assurance

Chelated DS-8273a, both CHX-A″-DTPA-DS-8273a and Df-Bz-NCS-DS-8273a, were intact by SDS-PAGE analysis under reducing and non-reducing conditions (data not shown). DS-8273a chelated with CHX-A″-DTPA was radiolabeled with ^{111}In at an efficiency of 47.27 ± 10.18 %, high radiochemical purity (99.7 ± 0.34 %, Fig. S1A) and immunoreactivity of 97.67 ± 4.04 % (Fig. 1A). Specific activity was 1.46 ± 0.18 mCi/mg protein. In comparison, DS-8273a chelated with Df-Bz-NCS was radiolabeled with ^{89}Zr at an efficiency of 82.56 ± 7.66 %, and high radiochemical purity (98.20 ± 1.64 %, Fig. S1B) and immunoreactivity of 97.07 ± 5.08 % (Fig. 1B). Specific activity was 1.49 ± 0.11 mCi/mg protein. Data was also obtained for stability of ^{111}In-CHX-A″-DTPA-DS-8273a (purity, 99.1%; immunoreactivity, 82.3%) and ^{89}Zr-Df-Bz-NCS-DS-8273a (purity, 98.3%; immunoreactivity, 80.5%), after 7 days in human serum. Chelator:antibody ratios for CHX-A″-DTPA-DS-8273a and Df-Bz-NCS-DS-8273a were determined at 3:1 and 1:1 respectively via ESI-MS (Supplementary Materials and Methods, Fig. S2-S4).

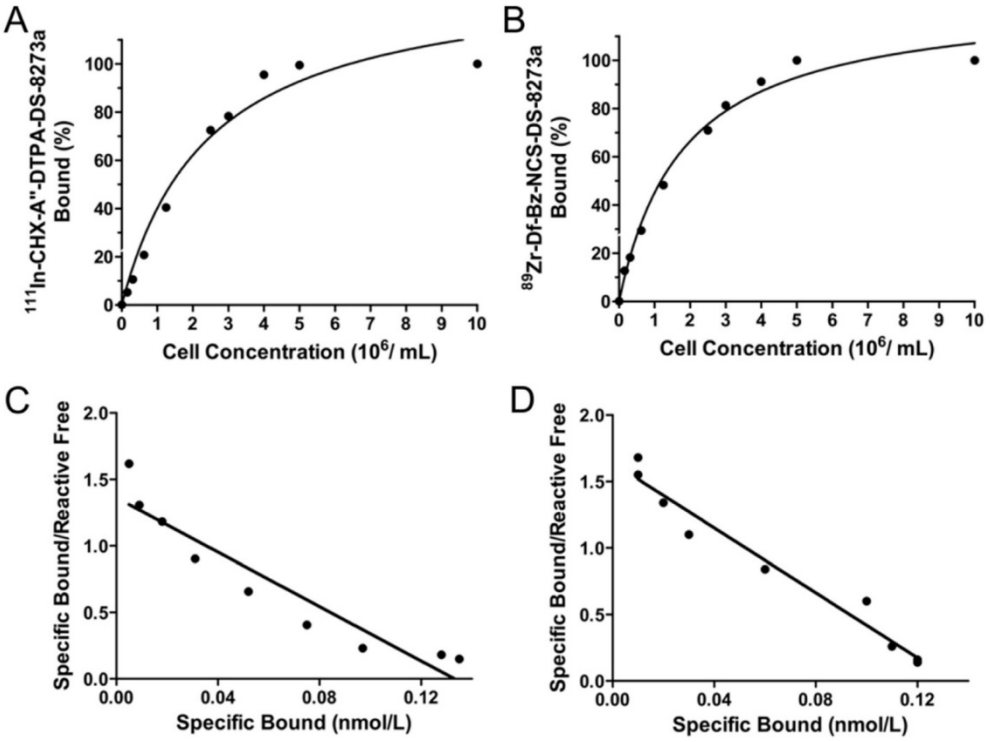

Figure 1: *In vitro* binding assays with radiolabeled DS-8273a. Lindmo plots showing binding of (A) ^{111}In-CHX-A″-DTPA-DS-8273a and (B) ^{89}Zr-Df-Bz-NCS-DS-8273a to increasing concentrations of DR5-positive COLO 205 cells. Scatchard plot of (C) ^{111}In-CHX-A″-DTPA-DS-8273a and (D) ^{89}Zr-Df-Bz-NCS-DS-8273a to COLO 205 cells.

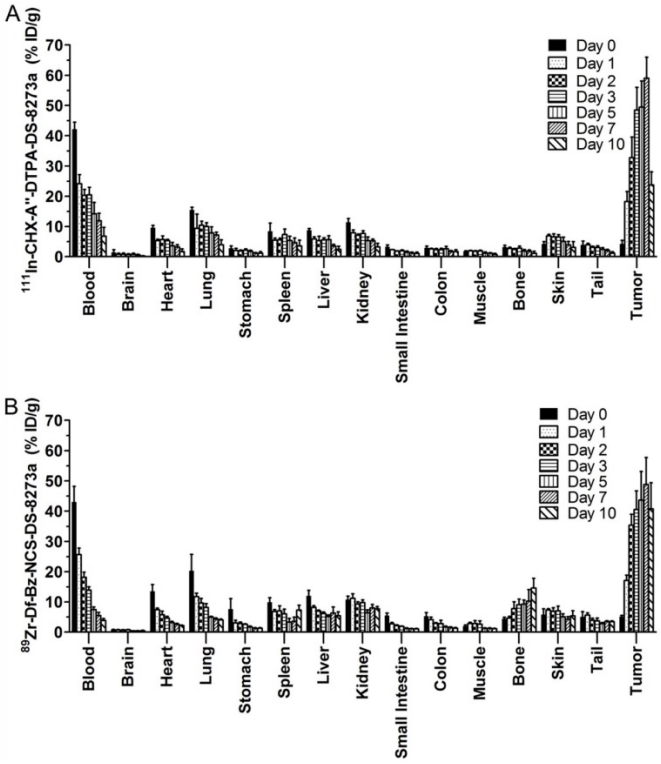

Figure 2: Biodistribution properties of (A) ^{111}In-CHX-A″-DTPA-DS-8273a and (B) ^{89}Zr-Df-Bz-NCS-DS-8273a in COLO 205 xenografted BALB/c *nu/nu* mice over 10 days (*bars*; mean ± SD; *n* = 5).

Scatchard analysis indicates that the ^{111}In-conjugate has an apparent K_a of 1.02×10^{10} M^{-1} and the number of antibody binding sites per cell is approximately 32,000 (Fig. 1C). In comparison, the ^{89}Zr-conjugate has an apparent K_a of 1.22×10^{10} M^{-1} and the number of antibody binding sites per cell is approximately 32,000 (Fig. 1D).

Biodistribution Studies of ^{111}In- and ^{89}Zr-labeled DS-8273a in COLO 205 tumor-bearing mice

Figure 2 summarizes the biodistribution results of ^{111}In-CHX-A″-DTPA-DS-8273a and ^{89}Zr-Df-Bz-NCS-DS-8273a in DR5-positive COLO 205 tumors. Both ^{111}In- and ^{89}Zr-labeled DS-8273a demonstrated high tumor uptake in DR5-positive tumors. No significant differences in tumor uptake was observed, with the exception of tumor uptake on day 10 post injection (mean ± SEM %ID/g; ^{111}In-CHX-A″-DTPA-DS-8273a, 23.70 ± 1.950 %ID/g; ^{89}Zr-Df-Bz-NCS-DS-8273a, 40.74 ± 3.882; $P = 0.0776$).

The tumor-to-blood ratio increased from 0.102 ± 0.029 (day 0) to 5.198 ± 1.323 (day 7) with ^{111}In-labeled DS-8273a and from 0.40 ± 0.12 (day 0) to 8.94 ± 1.26 (day 7) with ^{89}Zr-labeled DS-8273a. Other normal tissues showed clearance patterns typical of the clearance of a radiolabeled antibody. There was some

minor bone uptake of ^{89}Zr-Df-Bz-NCS-DS-8273a, most likely due to ^{89}Zr-chelate localization.

Tumor uptake of radioconjugate in DR5-negative tumors, CT26, on day 2 post injection was significantly lower than COLO 205 both for the ^{111}In-conjugate and the ^{89}Zr-conjugate (^{111}In-, 8.76 ± 1.41 %ID/g versus 32.71 ± 6.86 respectively, P < 0.0001; ^{89}Zr-, 9.67 ± 1.56 %ID/g versus 35.38 ± 3.65 respectively, P < 0.0001) (Fig. 3). Higher uptake of radioconjugates in COLO 205 compared to antigen negative CT26 control tumors confirms that tumor targeting of DS-8273a was specific.

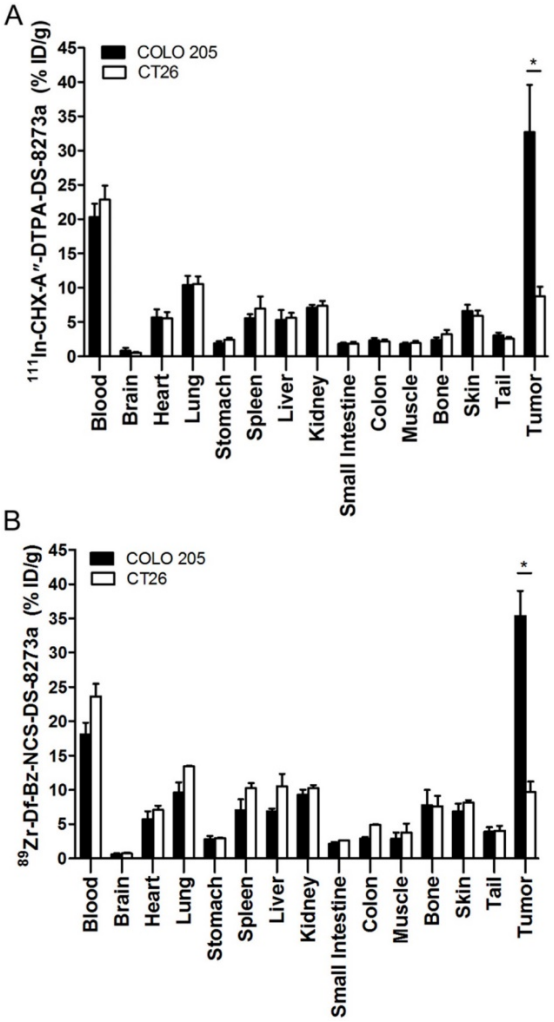

Figure 3: Biodistribution properties of (A) ^{111}In-CHX-A″-DTPA-DS-8273a and (B) ^{89}Zr-Df-Bz-NCS-DS-8273a in BALB/c *nu/nu* mice bearing DR5-positive COLO 205 xenografts versus DR5-negative CT26 mouse colon xenografts on day 2 after injection (bars, mean ± SD; n = 5, *, P < 0.0001).

In vivo molecular imaging of DR5 expression

Fused SPECT/CT images clearly indicate excellent uptake of ^{111}In-CHX-A″-DTPA-DS-8273a in a COLO 205 tumor in the left flank at the day 7 post injection (Fig. 4A). At this dose level (~4.8mg/kg), tumor shrinkage was seen between days 2 and 7 (data not shown), but ^{111}In-CHX-A″-DTPA-DS-8273a uptake in tumors was evident at the later time points despite the small sized tumors. No weight loss of mice was observed during the imaging period. Clearance of blood pool activity with time, and some liver uptake, is consistent with the pharmacokinetics and catabolic pathways of radiolabeled intact antibodies.

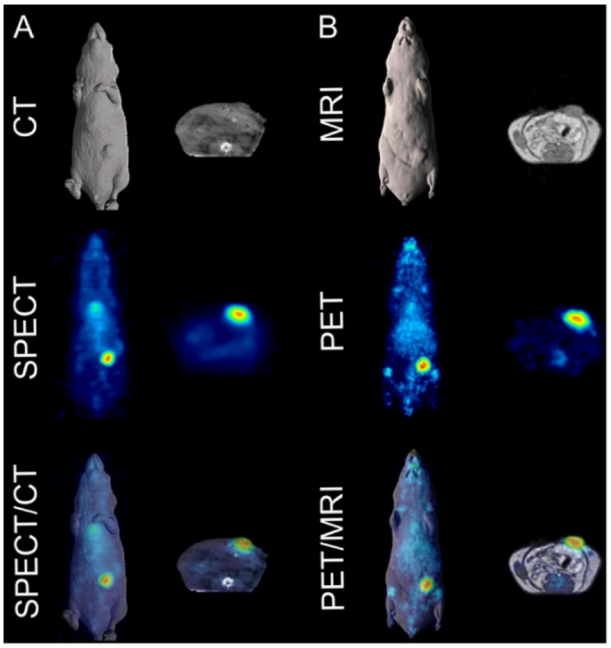

Figure 4: *In vivo* imaging of DR5 in COLO 205 xenografted mice. (A) Representative whole-body (*left*) and transaxial (*right*) images of CT (*top row*), SPECT (*middle row*) and fused SPECT/CT (*bottom row*) taken on day 7 post injections of ^{111}In-CHX-A″-DTPA-DS-8273a. (B) Representative whole-body (*left*) and transaxial (*right*) images of MRI (*top row*), PET (*middle row*) and fused PET/MRI (*bottom row*) taken on day 7 post injection of ^{89}Zr-Df-Bz-NCS-DS-8273a.

Similarly, whole body PET/MR images showed localization of ^{89}Zr-Df-Bz-NCS-DS-8273a to tumors in the left flank on day 7 post injection (Fig. 4B). Again, tumor shrinkage was seen between days 2 and 7 at this dose level (~3mg/kg) (Fig. S5), with maximum tumor growth inhibition seen on day 7 post injection (%TGI; 0.3 mg/kg, 27%; 3 mg/kg, 76%; 30mg/kg, 81%). Uptake of ^{89}Zr-Df-Bz-NCS-DS-8273a in tumors was clearly evident up to 7 days post injection. Some spleen and liver activity, and bone uptake, consistent with catabolism of ^{89}Zr-Df-Bz-NCS, was also observed.

In vivo DR5 receptor saturation

A combination study of biodistribution and PET/MRI explored the saturation of the DR5 receptor *in vivo*. A biodistribution study compared the organ uptake of ^{89}Zr-labeled DS-8273a (0.3 mg/kg) at different dose levels of unlabeled DS-8273a (0, 2.7 and 29.7 mg/kg) in mice bearing COLO 205 xenografts.

No significant differences were observed in blood and normal tissue biodistribution patterns (data not shown).

A protein dose effect was evident for COLO 205 tumor uptake. At all study time points, highest tumor uptake was observed at the 0.3 mg/kg DS-8273a dose, and lowest tumor uptake at 30 mg/kg, and significantly higher tumor-to-blood ratios were observed at 0.3 mg/kg protein dose compared to the 30 mg/kg dose over the duration of the study (Fig. 5).

Representative individual animal PET/MRI images of 0.3, 3 and 30 mg/kg ^{89}Zr-labeled DS-8273a on day 2 and 7 are shown in Fig. 6. COLO 205 tumor uptake of ^{89}Zr-labeled DS-8273a was clearly evident on day 2 (Fig. 6A) and day 7 (Fig. 6B) at all dose levels. Compared to the 0.3 mg/kg dose level, the 30 mg/kg DS-8273a dose level showed less uptake in the COLO 205 xenografts with time, consistent with the measured %ID/g levels and tumor-to-blood ratios as obtained from the biodistribution study (Fig. 5). Quantitative analysis of tumor volumes and tumor uptake confirmed a substantial reduction of tumor uptake at the higher dose levels compared to the 0.3 mg/kg dose level (Fig. 5).

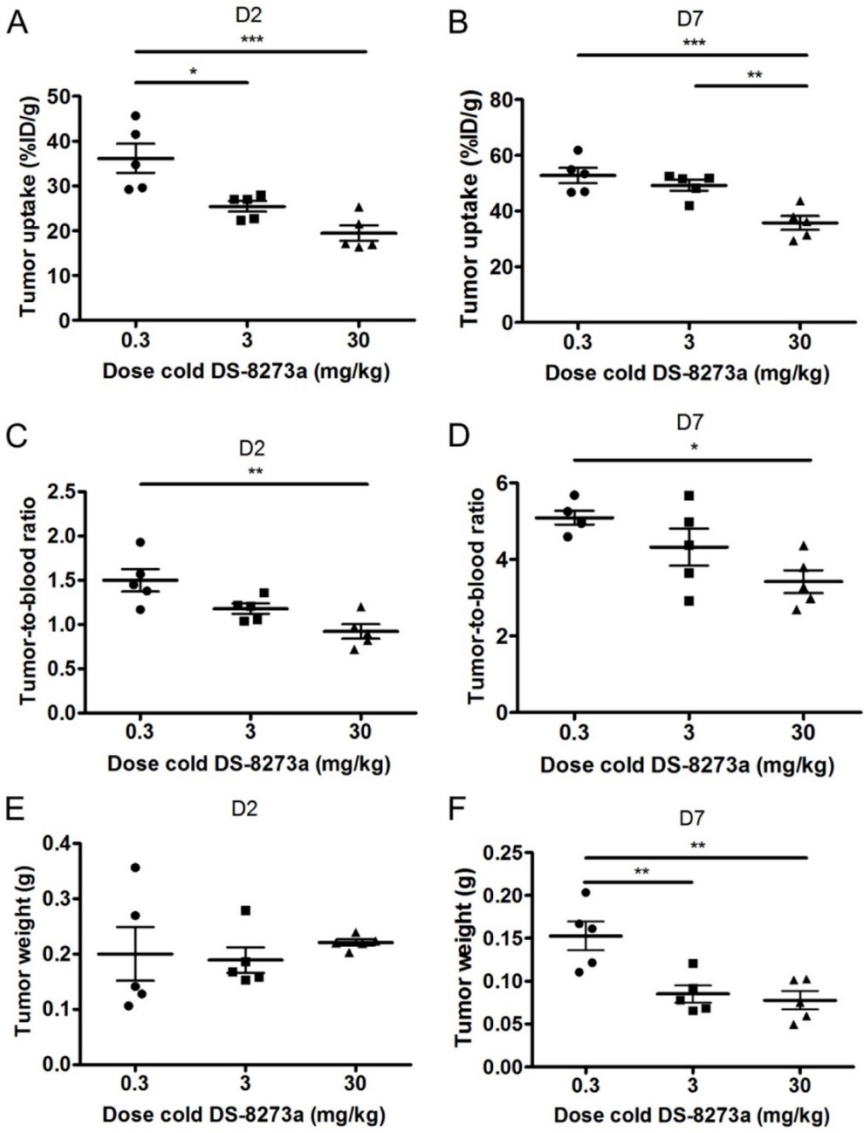

Figure 5: Influence of cold dose DS-8273a on tumor uptake of ^{89}Zr-Df-Bz-NCS-DS-8273a in BALB/c *nu/nu* mice bearing COLO 205 xenografts (A) on day 2 and (B) on day 7 post injection, and tumor-to-blood ratios (C) on day 2 and (D) on day 7 post injection. No significant differences were observed between average tumor sizes of each dose level (E) on day 2, but significant differences in tumor size were observed on day 7 post injection. *Bars*, SEM; $n = 5$. *, $P < 0.05$; **, $P < 0.005$; ***, $P < 0.0005$; ****, $P < 0.0001$.

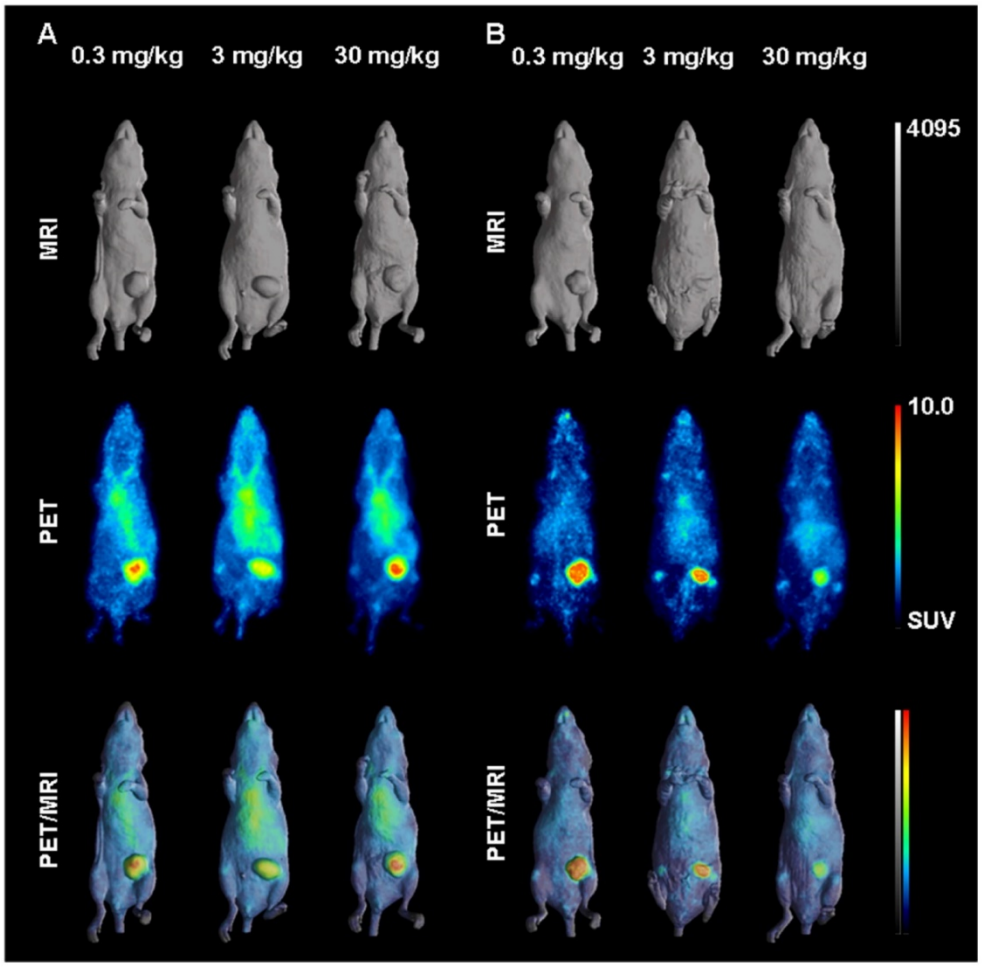

Figure 6: *In vivo* saturation of DR5 by ^{89}Zr-labeled DS-8273a demonstrated by PET/MR imaging at (A) day 2 and (B) day 7 post injection. Representative whole body surface-rendered MR images (*top*), maximum intensity projection PET images (*middle*) and fused PET/MR images (*bottom*) are shown for each time point at different dose levels of cold DS-8273a (0.3, 3 and 30 mg/kg).

Pharmacokinetics of ^{111}In- and ^{89}Zr-labeled DS-8273a

The mean pharmacokinetic parameters for ^{111}In- and ^{89}Zr-labeled DS-8273a administered at protein doses of 5 µg (0.3 mg/kg) are presented in Table 1. An unpaired t-test determined significant differences in the pharmacokinetic parameters between the two radioconjugates. ^{89}Zr-labeled DS-8273a showed a slightly faster clearance consistent with the higher tumor uptake observed with this radioconjugate.

Table 1: Pharmacokinetic parameters of ^{89}Zr- and ^{111}In-labeled DS-8273a.

Parameters	^{89}Zr-labeled DS-8273a*	^{111}In-labeled DS-8273a	*P*-value†
AUC (h × µg/mL)	172.33 ± 21.57	261.14 ± 21.56	0.0002
$t_{½\alpha}$ (h)	14.61 ± 8.53	1.95 ± 0.28	0.0294
$t_{½\beta}$ (h)	106.17 ± 49.42	126.74 ± 15.04	0.0244
C_{max} (µg/mL)	2.49 ± 0.23	3.10 ± 0.09	0.0033
C_L (mL/h)	0.029 ± 0.004	0.019 ± 0.002	< 0.0001
V_{ss} (mL)	3.54 ± 0.86	3.44 ± 0.18	0.1845 (*ns*)

Abbreviations: AUC, area under the curve; $t_{½\alpha}$, half-life of initial phase disposition; $t_{½\beta}$ half-life of the terminal phase of disposition; C_{max}, maximum plasma-serum concentration; C_L, total serum clearance; V_{ss}, volume of distribution at steady state; *ns*, not significantly different

*Data presented as mean ± SD (n = 5); †, Results of an unpaired t-test, Welch's correction was used when variances were significantly different

Discussion

In this study, DS-8273a, an anti-DR5 antibody, was successfully radiolabeled with ^{111}In for SPECT scanning, and ^{89}Zr for PET molecular imaging. Chelation and radiolabeling did not alter the structural integrity or immunoreactivity of the constructs. These constructs were stable in plasma for up to 7 days and demonstrated specific uptake in DR5-postitive COLO 205 tumors.

We demonstrated that DS-8273a had a higher affinity for DR5 compared to the first generation DR5 antibody CS-1008. Higher affinities were observed for ^{111}In-CHX-A″-DTPA-DS-8273a (K_a; 1.22 × 10^{10} M^{-1}) and ^{89}Zr-Df-Bz-NCS-DS-8273a (K_a; 1.02 × 10^{10} M^{-1}) compared to ^{111}In-CHX-A″-DTPA-CS-1008 (5.4 × 10^8

M^{-1}) [13]. Similarly, *in vivo* data showed that ^{111}In-CHX-A″-DTPA-DS-8273a and ^{89}Zr-Df-Bz-NCS-DS-8273a had higher COLO 205 tumor uptake and retention compared to ^{111}In-CHX-A″-DTPA-CS-1008 [13].

There were minimal differences between the two conjugates of DS-8273a in comparative *in vitro* and *in vivo* studies. Tumor uptake of the ^{111}In- and the ^{89}Zr-DS-8273a conjugate were similar with no significant differences in tumor uptake observed, with the exception of tumor uptake on day 10 p.i. (mean ± SEM %ID/g; ^{111}In-CHX-A″-DTPA-DS-8273a, 23.70 ± 1.950 %ID/g; ^{89}Zr-Df-Bz-NCS-DS-8273a, 40.74 ± 3.882; P = 0.0776). The slightly higher bone uptake seen with ^{89}Zr-Df-Bz-NCS-DS-8273a is a result of catabolized free ^{89}Zr, and similar to that seen with other ^{89}Zr-labeled antibodies [15, 16]. Both ^{111}In- and ^{89}Zr-radiolabeled DS-8273a showed high, specific and prolonged tumor uptake in animal models comparable to other ^{111}In-labeled and ^{89}Zr-labeled antibodies (e.g. hu3S193 and Herceptin®), despite the much higher expression of antigens such as Lewis Y and ERBB2 on tumor cell surface [15-19].

A murine colon cancer cell line, CT26, was used as a negative control in xenograft studies. DS-8273a does not recognize murine DR5. Although CT26 does present a true negative control due to the absence of human DR5, some limitations of this model are that syngeneic tumors might have a different micro-environmental architecture compared to human xenografts, which could influence biodistribution, and the absence of human DR5 expression in normal tissues does not reflect normal human DR5 expression in normal tissues. However, previous studies published with CS-1008 show that DR5 uptake in this mouse model is relevant to the human scenario [13, 14] as the clinical trial of ^{111}In-CHX-A″-DTPA-CS-1008 showed no uptake in normal tissue. Therefore, the use of CT26 as a negative tumor control is justified.

The impact of protein dose on ^{89}Zr-Df-Bz-NCS-DS-8273a biodistribution and tumor uptake was also investigated in a combined biodistribution and PET/MRI study, where reduced tumor uptake of trace radiolabeled ^{89}Zr-Df-Bz-NCS-DS-8273a (0.3 mg/kg) was observed in the presence of 3 mg/kg and 30 mg/kg cold DS-8273a on day 2 and day 7 p.i. Comparison of non-specific tumor uptake of trace radiolabeled ^{89}Zr-Df-Bz-NCS-DS-8273a (0.3 mg/kg) in DR5-negative CT26 tumors versus specific tumor uptake of radiolabeled ^{89}Zr-Df-Bz-NCS-DS-8273a in COLO 205 tumors at different dose levels (0.3, 3 and 30 mg/kg) suggests that the DR5 occupancy is affected by higher protein dose levels, but saturation is not completely reached at the 30 mg/kg dose level. This might be the result of the DS-8273a concentration in the tumor gradually increasing with time and some DR5 turnover. In addition, a clear anti-tumor response was visible in the time course of the imaging study, which was not evident at similar protein dose levels in prior studies of CS-1008, indicating the potent apoptosis inducing effects of DS-8273a *in vivo*.

These results have direct relevance to the design and conduct of DS-8273a clinical trials in cancer patients. As PET imaging allows for high resolution imaging in patients, and both radioconjugates demonstrate similar characteristics in preclinical studies, ^{89}Zr-Df-Bz-NCS-DS-8273a is our lead compound for a first-in-man clinical bioimaging study. There is direct clinical relevance of these findings as we have previously shown in several first-in-man clinical bioimaging studies that there is an excellent correlation between preclinical and clinical biodistribution data and gamma camera imaging using radiolabeled monoclonal antibodies [14, 20-23].

In conclusion, we have shown that DS-8273a is a highly potent DR5 agonistic antibody, and superior to CS-1008 in preclinical models. ^{89}Zr-Df-Bz-NCS-DS-8273a provides non-invasive quantitative imaging of DR5 expression, and PET imaging of DR5 expression will provide important quantitative information in planned human trials.

Supplementary Material

Supplementary figures.
http://www.thno.org/v06p2225s1.pdf

Abbreviations

AUC: area under the curve; CHX-A″-DTPA: C-functionalized *trans*-cyclohexyldiethylenetriamine-pentaacetic acid; C_{max}: maximum plasma-serum concentration; C_L: total serum clearance; CT: computed tomography; Df-Bz-NCS: *p*-isothiocyanatobenzyl-desferrioxamine; DR5: death receptor 5; ERBB2: receptor tyrosine-protein kinase erbB-2; %ID/g: percent injected dose per gram of tissue; kBq: kilobecquerel; MBq: megabecquerel; MRI: magnetic resonance imaging; MTD: maximum tolerated dose; SEC: size exclusion chromatography; SPECT: single photon emission computed tomography; $t_{½\alpha}$: half-life of initial phase disposition; $t_{½\beta}$: half-life of the terminal phase of disposition; TRAIL: TNF-related apoptosis-inducing ligand; PBS: phosphate-buffered saline; PET: positron emission tomography; p.i.: post injection; VOI: volume of interest; V_{ss}: volume of distribution at steady state.

Acknowledgement

The authors acknowledge the Australian Cancer Research Foundation for providing funds to purchase the PET/MRI and nanoSPECT/CT imaging equipment and the Operational Infrastructure Support program of the Victorian State Government. This research was also undertaken using the Solid Target Laboratory, an ANSTO-Austin-LICR Partnership.

Competing Interests

Masakatsu Kotsuma, Toshiaki Ohtsuka and Giorgio Senaldi are employees of Daiichi Sankyo Co. Ltd. This work was supported by funding from Daiichi Sankyo Co. Ltd.

References

1. Walczak H, Degli-Esposti MA, Johnson RS, Smolak PJ, Waugh JY, Boiani N, et al. TRAIL-R2: a novel apoptosis-mediating receptor for TRAIL. EMBO J. 1997; 16: 5386-97.
2. Takeda K, Stagg J, Yagita H, Okumura K, Smyth MJ. Targeting death-inducing receptors in cancer therapy. Oncogene. 2007; 26: 3745-57.
3. Lemke J, von Karstedt S, Zinngrebe J, Walczak H. Getting TRAIL back on track for cancer therapy. Cell Death Differ. 2014; 21: 1350-64.
4. Holland PM. Death receptor agonist therapies for cancer, which is the right TRAIL? Cytokine & growth factor reviews. 2014; 25: 185-93.
5. de Miguel D, Lemke J, Anel A, Walczak H, Martinez-Lostao L. Onto better TRAILs for cancer treatment. Cell Death Differ. 2016; 23: 733-47.
6. Koornstra JJ, Kleibeuker JH, van Geelen CM, Rijcken FE, Hollema H, de Vries EG, et al. Expression of TRAIL (TNF-related apoptosis-inducing ligand) and its receptors in normal colonic mucosa, adenomas, and carcinomas. J Pathol. 2003; 200: 327-35.
7. Van Geelen CM, de Vries EG, de Jong S. Lessons from TRAIL-resistance mechanisms in colorectal cancer cells: paving the road to patient-tailored therapy. Drug Resist Updat. 2004; 7: 345-58.
8. Yada A, Yazawa M, Ishida S, Yoshida H, Ichikawa K, Kurakata S, et al. A novel humanized anti-human death receptor 5 antibody CS-1008 induces apoptosis in tumor cells without toxicity in hepatocytes. Ann Oncol. 2008; 19: 1060-7.
9. Ichikawa K, Liu W, Zhao L, Wang Z, Liu D, Ohtsuka T, et al. Tumoricidal activity of a novel anti-human DR5 monoclonal antibody without hepatocyte cytotoxicity. Nat Med. 2001; 7: 954-60.
10. Lawrence D, Shahrokh Z, Marsters S, Achilles K, Shih D, Mounho B, et al. Differential hepatocyte toxicity of recombinant Apo2L/TRAIL versions. Nat Med. 2001; 7: 383-5.
11. Mori E, Thomas M, Motoki K, Nakazawa K, Tahara T, Tomizuka K, et al. Human normal hepatocytes are susceptible to apoptosis signal mediated by both TRAIL-R1 and TRAIL-R2. Cell Death Differ. 2004; 11: 203-7.
12. Forero-Torres A, Shah J, Wood T, Posey J, Carlisle R, Copigneaux C, et al. Phase I trial of weekly tigatuzumab, an agonistic humanized monoclonal antibody targeting death receptor 5 (DR5). Cancer Biother Radiopharm. 2010; 25: 13-9.
13. Burvenich IJ, Lee FT, Cartwright GA, O'Keefe GJ, Makris D, Cao D, et al. Molecular imaging of death receptor 5 occupancy and saturation kinetics in vivo by humanized monoclonal antibody CS-1008. Clin Cancer Res. 2013; 19: 5984-93.
14. Ciprotti M, Tebbutt NC, Lee FT, Lee ST, Gan HK, McKee DC, et al. Phase I Imaging and Pharmacodynamic Trial of CS-1008 in Patients With Metastatic Colorectal Cancer. J Clin Oncol. 2015; 33: 2609-16.
15. Dijkers EC, Kosterink JG, Rademaker AP, Perk LR, van Dongen GA, Bart J, et al. Development and characterization of clinical-grade 89Zr-trastuzumab for HER2/neu immunoPET imaging. J Nucl Med. 2009; 50: 974-81.
16. Holland JP, Divilov V, Bander NH, Smith-Jones PM, Larson SM, Lewis JS. 89Zr-DFO-J591 for immunoPET of prostate-specific membrane antigen expression in vivo. J Nucl Med. 2010; 51: 1293-300.
17. Lee FT, Rigopoulos A, Hall C, Clarke K, Cody SH, Smyth FE, et al. Specific localization, gamma camera imaging, and intracellular trafficking of radiolabelled chimeric anti-G(D3) ganglioside monoclonal antibody KM871 in SK-MEL-28 melanoma xenografts. Cancer Res. 2001; 61: 4474-82.
18. Clarke K, Lee FT, Brechbiel MW, Smyth FE, Old LJ, Scott AM. In vivo biodistribution of a humanized anti-Lewis Y monoclonal antibody (hu3S193) in MCF-7 xenografted BALB/c nude mice. Cancer Res. 2000; 60: 4804-11.
19. Janjigian YY, Viola-Villegas N, Holland JP, Divilov V, Carlin SD, Gomes-DaGama EM, et al. Monitoring afatinib treatment in HER2-positive gastric cancer with 18F-FDG and 89Zr-trastuzumab PET. J Nucl Med. 2013; 54: 936-43.
20. Scott AM, Lee FT, Tebbutt N, Herbertson R, Gill SS, Liu Z, et al. A phase I clinical trial with monoclonal antibody ch806 targeting transitional state and mutant epidermal growth factor receptors. Proc Natl Acad Sci U S A. 2007; 104: 4071-6.
21. Scott AM, Lee FT, Jones R, Hopkins W, MacGregor D, Cebon JS, et al. A phase I trial of humanized monoclonal antibody A33 in patients with colorectal carcinoma: biodistribution, pharmacokinetics, and quantitative tumor uptake. Clin Cancer Res. 2005; 11: 4810-7.
22. Herbertson RA, Tebbutt NC, Lee FT, MacFarlane DJ, Chappell B, Micallef N, et al. Phase I biodistribution and pharmacokinetic study of Lewis Y-targeting immunoconjugate CMD-193 in patients with advanced epithelial cancers. Clin Cancer Res. 2009; 15: 6709-15.
23. Herbertson RA, Tebbutt NC, Lee FT, Gill S, Chappell B, Cavicchiolo T, et al. Targeted chemoradiation in metastatic colorectal cancer: a phase I trial of 131I-huA33 with concurrent capecitabine. J Nucl Med. 2014; 55: 534-9.